

Warm Hybrid Axion Inflation in α -Attractor Models Constrained by ACT and Future Plan experiments.

Waqas Ahmed^{1*}, Waqar Ahmad^{2,4†}, Ahsan Illahi^{3‡} M. Junaid^{4§}

¹ *Center for Fundamental Physics, School of Artificial Intelligence, Hubei Polytechnic University, Huangshi 435003, China.*

² *School of Natural Sciences, Department of Physics and Astronomy, National University of Sciences and Technology, Islamabad, Pakistan.*

³ *Department of Physics, COMSATS University Islamabad, Islamabad, Pakistan.*

⁴ *National Centre for Physics, Islamabad, Pakistan.*

We present a comprehensive study of warm hybrid inflation within the framework of α -attractor models, where an axionic inflaton is coupled to a waterfall field in the presence of thermal dissipation. The model is analyzed for both linear ($\Upsilon \propto T$) and cubic ($\Upsilon \propto T^3$) dissipation regimes. Confronting the theoretical predictions with the latest observational data from Planck+BICEP/Keck, P-ACT-LB-BK18 and SPT, and , we find that in the weak dissipative regime ($Q_* \lesssim 10^{-5}$), the scalar spectral index $n_s \simeq 0.965$ lies at the boundary of the combined P-ACT-LB-BK18 constraints, while the tensor-to-scalar ratio r remains within observable ranges. For stronger dissipation ($Q_* \gtrsim 10^{-5}$), the model predicts values of n_s well within the $1-2\sigma$ confidence region of all datasets, with tensor modes remaining fully observable in both dissipation scenarios. These results indicate that forthcoming CMB polarization experiments may be capable of detecting primordial gravitational waves, thereby providing a robust observational test of warm hybrid inflation across different dissipative regimes.

I. INTRODUCTION

Inflationary cosmology stands as the cornerstone of modern earl universe theory, providing a robust, predictive framework that explains the remarkable homogeneity, isotropy, and flatness of the observable universe[1, 2]. Inflation provides a beautiful solution to the traditional horizon and flatness problems of the Hot Big Bang model by proposing a phase of faster, quasi-exponential growth fuelled by the potential energy of an inflaton field, a scalar field. Most importantly, it also provides a quantum-mechanical mechanism by which the primordial density perturbations which flattened the cosmic microwave background (CMB) anisotropies and the universe in general were seeded to occur[3].

The success of inflation, however, is tempered by a fundamental theoretical challenge: the transition from a compelling cosmological paradigm to a concrete model grounded in particle physics. The central obstacle is the so-called eta-problem: maintaining the requisite flatness of the inflaton potential over super-Planckian field ranges while protecting it from large quantum corrections that would otherwise spoil the slow-roll conditions [4, 5]. This problem is exacerbated by the swampland conjectures in quantum gravity, which question the viability of sustained slow-roll inflation in regimes controlled by effective field theories weakly coupled to gravity [6, 7].

Traditionally, model building has sought refuge in symmetries such as supersymmetry or shift symmetries of pseudo-Nambu Goldstone bosons (axions) to protect the inflationary potential [8, 9]. However, these approaches often introduce their own fine-tuning problems or come into tension with observational bounds and theoretical constraints, such as the Weak Gravity Conjecture [10, 11]. Furthermore, recent advances in precision cosmology have rendered many simple and well-motivated particle physics models including monomial chaotic inflation scenarios with potentials $V(\phi) \propto \phi^2$ or $V(\phi) \propto \phi^4$, as well as attractor-type models such as Starobinsky and Higgs inflation—increasingly disfavored by observational data [12, 13].

This tension is starkly highlighted by the evolving observational landscape. Early data from the *Planck* satellite, combined with constraints from BICEP/Keck (BK), pointed to a scalar spectral index of

$$n_s \simeq 0.9652 \pm 0.0084 \quad (95\% \text{ CL}),$$

as reported in Refs. [14, 15]. However, more recent multi-experiment analyses have shifted the preferred value of n_s toward higher values. In particular, the so-called P-ACT-LB-BK18 dataset combining Data Release 6 from the Atacama Cosmology Telescope (ACT), *Planck*, BICEP/Keck, and DESI baryon acoustic oscillation measurements

* E-mail: waqasmit@hbpu.edu.cn

† E-mail: waqarahmad262@gmail.com

‡ E-mail: ahsanillahi@comsats.edu.pk

§ E-mail: mjunaid@ualberta.ca

yields

$$n_s = 0.9743 \pm 0.0068 \quad (95\% \text{ CL} : 0.967 \lesssim n_s \lesssim 0.981),$$

as shown in Refs. [13, 16, 17]. Meanwhile, an independent combination of South Pole Telescope (SPT), *Planck*, and ACT data (P-ACT-SPT) favors

$$n_s = 0.9684 \pm 0.006 \quad (95\% \text{ CL} : 0.962 \lesssim n_s \lesssim 0.974),$$

as reported in Ref. [18]. This upward trend in n_s , together with increasingly stringent upper limits on the tensor-to-scalar ratio,

$$r < 0.036 \quad (95\% \text{ CL}),$$

This poses a significant challenge to many canonical “cold” inflationary scenarios. In this context, numerous studies have recently investigated cold inflationary models, both within supersymmetric and non-supersymmetric frameworks, in light of observational constraints from the Atacama Cosmology Telescope (ACT); see Refs. [12, 19? –33]. These developments in cold inflation, particularly in explaining the P-ACT-LB-BK18 and SPT observations, also motivate us to explore axion hybrid inflation within the framework of warm inflation, which is itself well motivated, and to examine these results in this broader context [34, 35].

A promising and theoretically well-motivated path forward is provided by the paradigm of *warm inflation* (WI) [36, 37]. In contrast to standard “cold” inflation (CI), where the inflaton is assumed to be dynamically isolated from other degrees of freedom until a post-inflationary reheating phase, WI posits that sizable dissipative interactions between the inflaton and a thermal bath are already active during the inflationary era. These interactions are characterized by a dissipation coefficient Υ , which introduces an additional friction term $\Upsilon\dot{\phi}$ in the inflaton equation of motion. As a result, energy is continuously transferred from the inflaton to radiation, maintaining a non-negligible radiation energy density ρ_r throughout inflation.

This simple yet profound physical ingredient leads to several important consequences. First, it alleviates the η -problem: in the strong dissipative regime,

$$Q \equiv \frac{\Upsilon}{3H} \gg 1, \quad (1)$$

slow-roll evolution can be sustained even if quantum corrections generate an inflaton mass m_ϕ larger than the Hubble scale H , a situation that is incompatible with CI [38]. Second, WI naturally yields a smooth and graceful exit into a radiation-dominated universe without requiring a separate reheating phase [39]. Third, and most relevant for current observations, the dissipative dynamics and associated thermal fluctuations significantly modify the primordial power spectrum.

In warm inflation, the scalar curvature power spectrum receives enhanced contributions from thermal noise. It can be written as [40]

$$\mathcal{P}_R(k) = \left(\frac{H^2}{2\pi\dot{\phi}} \right)^2 F, \quad (2)$$

where the enhancement factor F is given by

$$F = \left(1 + 2n_* + \frac{2\sqrt{3}\pi Q}{\sqrt{3 + 4\pi Q}} \frac{T}{H} \right) G(Q). \quad (3)$$

Here, n_* accounts for the possible thermalization of inflaton fluctuations, while $G(Q)$ encodes the growth of perturbations due to the coupling between inflaton and radiation fluctuations and depends on the microphysical structure of the dissipation coefficient Υ [34].

These modifications can naturally yield a scalar spectral index n_s closer to unity and suppress the tensor-to-scalar ratio r , in excellent agreement with the trends favored by recent P-ACT-LB-BK18 and SPT observations [13].

Recent advances in numerical analysis, particularly through dedicated codes such as `WI2easy` [41], now enable precision calculations of both the background dynamics and cosmological perturbations in unified warm little inflaton (WLI) models. These studies demonstrate that the strong dissipative regime,

$$Q \gg 1, \quad (4)$$

of the combined framework is not only theoretically well motivated—ensuring sub-Planckian field excursions, $\Delta\phi < M_{\text{Pl}}$, and avoiding potential swampland constraints [42, 43] but is also explicitly favored by the preference for a higher scalar spectral index n_s indicated by the combined P-ACT-LB-BK18 data sets [13, 16]. Moreover, warm inflation naturally accommodates a mildly positive running of the scalar spectral index,

$$\alpha_s > 0, \quad (5)$$

as suggested by recent observations, a feature that remains challenging to realize within many cold inflation scenarios.

Motivated by these results, the present work aims to explore a related yet complementary direction: the incorporation of warm inflationary dynamics within the framework of hybrid inflation [44, 45]. Conventional hybrid inflation models, which employ a two-field mechanism to terminate inflation, typically neglect the potential role of sustained thermal effects during the inflationary phase. By combining the warm inflation paradigm with a hybrid structure with axionic background we seek to construct a robust and microphysically consistent inflationary scenario.

Our objective is to elucidate how the interplay between dissipative thermal friction, multi-field dynamics influences the inflationary observables, the reheating dynamics, and the connection to fundamental energy scales. To this end, we perform both analytical and numerical explorations of the model's parameter space, confronting its predictions for the scalar spectral index n_s , the tensor-to-scalar ratio r and the running α_s with the stringent constraints arising from the combined analyses of *Planck+BICEP/Keck*, P-ACT-LB-BK18 and SPT data. In doing so, we aim to contribute toward building a principled and observationally viable bridge between inflationary cosmology and high-energy fundamental physics.

The rest of the work is structured in the following manner. In Section II we introduce the theoretical framework of warm hybrid axion inflation in the framework of the α -attractor formalism, including the two-field potential, axionic self-interactions, and the warm inflation background equations. Section III outlines the dynamics of warm inflation, dissipation regimes, and the analytical formulation for cosmological perturbations. Section IV contains our comprehensive numerical analysis, exploring the full parameter space and presenting results for n_s , r , α_s , and T_*/H_* as functions of the dissipation ratio Q_* , along with a comparison to current observational datasets. Finally, in Section V, we summarize the key findings and conclude the work.

II. HYBRID INFLATION WITH AXION SECTOR

We investigate a hybrid warm inflation scenario involving axions (or axion-like particles), where the scalar field ϕ plays the role of the inflaton while ψ acts as the waterfall field. Unlike the standard cold picture, here the inflaton evolves in the presence of a thermal radiation bath maintained through dissipative processes. Additionally, we consider a non-canonical modification of the kinetic term of ϕ within the framework of an α -attractor model. The resulting Lagrangian density is [46]

$$L \simeq \frac{(\partial^\mu\phi)^2}{2\left(1 - \frac{\phi^2}{6\alpha}\right)^2} + \frac{(\partial^\mu\psi)^2}{2} - V(\phi, \psi), \quad (6)$$

where warm inflation effects are introduced through a dissipation coefficient $\Upsilon(\phi, T)$ that transfers inflaton energy to a thermal bath which we discuss in detail next section. The background evolution equations are modified as

$$\ddot{\phi} + (3H + \Upsilon)\dot{\phi} + V_\phi = 0, \quad \dot{\rho}_r + 4H\rho_r = \Upsilon\dot{\phi}^2, \quad (7)$$

where ρ_r is the radiation energy density.

The scalar potential is chosen as

$$V(\phi, \psi) = \kappa^2 \left(M^2 - \frac{\psi^2}{4}\right)^2 + V(\phi) + \frac{\lambda^2}{4}\phi^2\psi^2, \quad (8)$$

with the axionic self-interaction given by

$$V(\phi) = f^2 m^2 \left[1 - \cos\left(\frac{\phi}{f}\right)\right]. \quad (9)$$

Here M and m denote mass scales associated with the waterfall and inflaton sectors, respectively, while f is the axion decay constant and κ, λ are dimensionless couplings. In the warm inflation regime, the presence of dissipation

slows the evolution of ϕ near the critical point, causing the tachyonic instability of ψ to grow gradually rather than abruptly.

The parameter α originates from the hyperbolic geometry of α -attractor models [47, 48]. The associated kinetic term exhibits a pole at $\phi = \sqrt{6\alpha}$, stretching the potential in the canonical field frame and modifying inflationary observables such as n_s and r . Similar kinetic structures can also arise from renormalization group effects in Higgs sector extensions [49]. Introducing the canonical inflaton field via

$$\phi \rightarrow \sqrt{6\alpha} \tanh\left(\frac{\varphi}{\sqrt{6\alpha}}\right), \quad (10)$$

the hybrid potential becomes

$$V(\psi, \varphi) = \kappa^2 \left(M^2 - \frac{\psi^2}{4} \right)^2 + m^2 f^2 \left[1 - \cos \left(\frac{\sqrt{6\alpha} \operatorname{Tanh}\left(\frac{\varphi}{\sqrt{6\alpha}}\right)}{f} \right) \right] + \frac{\lambda^2}{2} \psi^2 \left(\sqrt{6\alpha} \operatorname{Tanh}\left(\frac{\varphi}{\sqrt{6\alpha}}\right) \right)^2. \quad (11)$$

The mass squared of the waterfall field at $\psi = 0$ is,

$$M_\psi^2 = \left(-\kappa^2 M^2 + \frac{1}{2} \left(\lambda \sqrt{6\alpha} \operatorname{Tanh}\left(\frac{\varphi}{\sqrt{6\alpha}}\right) \right)^2 \right). \quad (12)$$

To ensure stability along $\psi = 0$ during inflation, we assume

$$\frac{(\lambda \sqrt{6\alpha})^2}{2} > \kappa^2 M^2, \quad (13)$$

so that $M_\psi^2 > 0$ for $\varphi > \varphi_c$. The critical condition is

$$\operatorname{Tanh}^2\left(\frac{\varphi_c}{\sqrt{6\alpha}}\right) = \frac{V_0^{1/2}}{3\alpha\lambda_c}. \quad (14)$$

where $V_0 = \kappa^2 M^4$ and $\lambda_c = \lambda^2/\kappa$. Along the inflationary trajectory $\psi = 0$, the effective single-field potential becomes

$$V(\varphi) = V_0 + m^2 f^2 \left[1 - \cos \left(\frac{\sqrt{6\alpha} \operatorname{tanh}\left(\frac{\varphi}{\sqrt{6\alpha}}\right)}{f} \right) \right], \quad (15)$$

which drives the warm inflation dynamics together with the thermal bath. The resulting expressions for the scalar power spectrum, tensor-to-scalar ratio, and their dependence on the dissipation strength will be analyzed in subsequent sections.

III. WARM INFLATION

Warm inflation is the realization that the interactions between the inflaton and other fields as radiation can lead to dissipation of inflaton energy to other dynamical degrees of freedom. This means that particle production can occur concurrently with inflationary expansion as long as the scalar potential remains the dominant component of energy density in the universe, with the ambient temperature greater than the Hubble scale. Radiation can naturally come to dominate the energy density of the universe through this particle production without the need for the separate reheating phase of cold inflation[35, 50].

In the warm inflation scenario, inflaton interacts with other field(s) which is characterized by a dissipation coefficient. The evolution equation to govern the dynamics of warm inflaton field is

$$\ddot{\phi} + (3H + \Upsilon)\dot{\phi} + V_{,\phi} = 0 \quad (16)$$

where Υ is a dissipation coefficient, which is absent in the cold inflation. Whereas, the evolution of energy density can be extracted by invoking the energy conservation which reads as

$$\dot{\rho}_r + 4H\rho_r = \Upsilon\dot{\phi}^2 \quad (17)$$

The term $\Upsilon\dot{\phi}^2$ encodes the transfer of energy from the inflaton and the radiation bath. In warm inflation, it is assumed that the radiation to be thermalized:

$$\rho_r = (\pi^2/30)g^*T^4 \quad (18)$$

where g^* signifies the light degrees of freedom for the radiation bath. Finally, the Friedmann equation takes the following form:

$$H^2 = \frac{1}{3m_p^2} \left(\frac{\dot{\phi}^2}{2} + V(\phi) + \rho_r \right) \quad (19)$$

where $m_p = 1/\sqrt{8\pi G}$ is the reduced Planck mass.

In warm inflation slow roll approximations remain applicable. In slow-roll regime, where the 2nd order derivative of inflaton field, ϕ in Eq. 16 and 1st order derivative of energy density, ρ_r , in Eq. 17 can be neglected, the evolution equations for inflaton and energy densities turn to be

$$3H(1+Q)\dot{\phi} = -V'(\phi), \quad (20)$$

$$\rho_R = \frac{3}{4}Q\dot{\phi}^2 \quad (21)$$

$$Q = C_\phi T^p \phi^q M^{1-p-q}/3H \quad (22)$$

where C_ϕ is the dissipation coefficient and Q is the generalized dissipation coefficient ratio[51], which is dimensionless. The power of temperature T^p with $p = 1$ corresponding to linear and $p = 3$ as cubic dissipation regimes. In this study, we focus only on temperature dependence ignoring ϕ in the dissipation ratio, and hence we take $q = 0$. The dissipation ratio Q characterizes the efficiency of energy transfer from the inflaton field to the radiation bath. Its magnitude determines two distinct regimes of warm inflation: the *weak dissipative regime* (WDWI) when $Q \ll 1$ and the *strong dissipative regime* (SDWI) when $Q \gg 1$.

The slow roll parameters for warm inflation σ_V , η_V & ϵ_V are given by:

$$\epsilon_V = \frac{m_p^2}{2} \left(\frac{V_{,\phi\phi}}{V} \right)^2, \quad \eta_V = m_p^2 \frac{V_{,\phi\phi}}{V}, \quad \sigma_V = \frac{m_p^2 V_{,\phi}}{\phi V}. \quad (23)$$

$$\epsilon = \frac{\epsilon_V}{1+Q}, \quad \eta = \frac{\eta_V - \epsilon_V}{1+Q} \quad (24)$$

while the Hubble slow-roll parameters ϵ and η explicitly depend on the dissipation ratio Q .

The standard power spectrum for warm inflation is given by

$$P_s = \left(\frac{H_*^2}{2\pi m_p \dot{\phi}} \right)^2 \left(1 + 2n_{BE} + \frac{T_* 2\sqrt{3}\pi Q_*}{H_* \sqrt{3+4\pi Q_*}} \right) G(Q_*), \quad (25)$$

$$n_{BE} = \frac{1}{\exp\left(\frac{H_*}{T_*}\right) - 1}, \quad (26)$$

$$G(Q) = 1 + 4.981Q^{1.946} + 0.127Q^{4.33}, \quad (27)$$

$$n_s = 1 + \frac{\partial \ln P_s}{\partial \ln k} = 1 + (1-\epsilon)^{-1} \frac{\partial \ln P_s}{\partial \ln N}. \quad (28)$$

We use this basic definition of spectra where $G(Q)$ is called the growth factor and n_{BE} the Boltzmann statistics of the photon bath.

IV. NUMERICAL ANALYSIS

We perform a detailed numerical study of the warm hybrid axion inflation dynamics and compute the resulting primordial power spectra. The background evolution is governed by the coupled inflaton-radiation system in the

presence of a dissipative term $\Upsilon(T)$ arising from axion–gauge field interactions. To solve the system efficiently, we adopt dimensionless variables and use the number of e-folds N as the time variable [50]:

$$x = \phi/m_p, \quad y = \dot{\phi}, \quad z = m_p H, \quad r = \rho_r, \quad (29)$$

$$x_{,N} = y/z, \quad (30)$$

$$y_{,N} = -3(1+Q)y - V_{,x}/z, \quad (31)$$

$$r_{,N} = -4r + 3Qy^2, \quad (32)$$

$$z^2 = \frac{1}{3} \left(\frac{y^2}{2} + V(x) + r \right), \quad (33)$$

where $Q \equiv \Upsilon/(3H)$ is the dissipative ratio and $V(x)$ is the axion potential. The subscript $(,N)$ denotes a derivative with respect to N . We consider two temperature-dependent forms of the dissipation coefficient:

- **Linear dissipation:** $\Upsilon(T) \propto T$,
- **Cubic dissipation:** $\Upsilon(T) \propto T^3$,

which correspond to distinct microscopic regimes of axion–gauge field interactions [52].

All numerical solutions are obtained using the **WI2easy** Mathematica code [41], a dedicated solver for warm inflation dynamics that integrates the background equations (30–33) together with the perturbation equations for scalar and tensor modes. The scalar power spectrum P_s and tensor power spectrum P_t are computed using the generalized warm inflation formalism [53, 54]. The scalar spectral index n_s and tensor-to-scalar ratio r are evaluated at the pivot scale $k_* = 0.05 \text{ Mpc}^{-1}$. We calibrate the potential amplitude using the measured value of P_s from Planck [14], which also fixes T^*/H^* for each benchmark point. We have verified the consistency of our **WI2easy** results with other warm inflation solvers such as **WI-easy** [41] and ensured numerical convergence across the parameter space.

To systematically explore the model predictions, we select four benchmark points (BP1–BP4) that span the weak, intermediate, and strong dissipative regimes. Their parameters are listed in Table I. The main results are displayed

TABLE I: Parameters for the four benchmark points used in the numerical scan.

Benchmark	V_0	m/m_p	f/m_p	$V0_{\text{Linear}}$	$V0_{\text{Cube}}$
BP1	$V0 \times 10^{-10}$	$\sqrt{V0} \times 2.8 \times 10^{-6}$	100	0.015	0.021
BP2	$V0 \times 10^{-8}$	$\sqrt{V0} \times 2.8 \times 10^{-6}$	100	0.0086	0.0093
BP3	$V0 \times 10^{-10}$	$\sqrt{V0} \times 2.8 \times 10^{-6}$	10	0.0019	0.384
BP4	$V0 \times 10^{-10}$	$\sqrt{V0} \times 2.77 \times 10^{-6}$	1	0.782	0.813

in Fig. 1 top panel illustrates the relationship between the dissipation ratio Q_* and the thermal ratio T_*/H_* across the full parameter space, revealing a transition at $Q_* \simeq 3.5 \times 10^{-5}$. In the cold inflation regime ($Q_* < 3.5 \times 10^{-5}$), $T_*/H_* < 0.1$, implying that the thermal bath is negligible compared to the Hubble scale, and quantum fluctuations dominate.

In the transition region ($3.5 \times 10^{-5} < Q_*$), $0.1 < T_*/H_* < 1$, indicating that thermal effects are comparable to quantum effects. For the warm inflation regime ($Q_* > 10^{-5}$), $T_*/H_* > 1$, so thermal fluctuations dominate over quantum fluctuations and significantly affect the inflaton dynamics. The thermal transition behavior differs between linear ($\Upsilon \propto T$) and cubic ($\Upsilon \propto T^3$) dissipation forms. For linear dissipation, the transition is sharper at $Q_* \simeq 2.8 \times 10^{-5}$, thermalization occurs faster due to linear temperature dependence, and the correlation between the thermal ratio and dissipation is $T_*/H_* \propto Q_*^{0.85}$ for $Q_* > 10^{-4}$. In contrast, cubic dissipation shows a broader transition centered at $Q_* \simeq 4.2 \times 10^{-5}$, with slower initial thermalization but stronger temperature feedback, giving $T_*/H_* \propto Q_*^{0.45}$ for $Q_* > 10^{-4}$.

The bottom panel shows in Fig. 1, which shows the scalar spectral index n_s as a function of the dissipative ratio at horizon crossing Q_* for both linear (left panel) and cubic (right panel) dissipation cases. The colored curves correspond to the four benchmark points, and the shaded regions represent the 68% and 95% confidence levels from combined CMB datasets (Planck+BK18, P-ACT-LB-BK18, SPT).

In the limit $Q_* \rightarrow 0$, the model reduces to cold inflation. For all benchmarks, n_s asymptotically reaches a value $\approx (0.96 - 0.965)$, which may be in the preferred range of Planck $n_s = 0.9649 \pm 0.0042$ [14]. However, these results of cold inflation fall outside the combined Planck and ACT DR4/DR6 (TT+TE+EE) bounds in $n_s = 0.9743 \pm 0.01$. Thus, cold inflation is not best fit regime of our model, as it fails to match the observed spectral tilt of $n_s = 0.9743$ by P-ACT-LB-BK18.

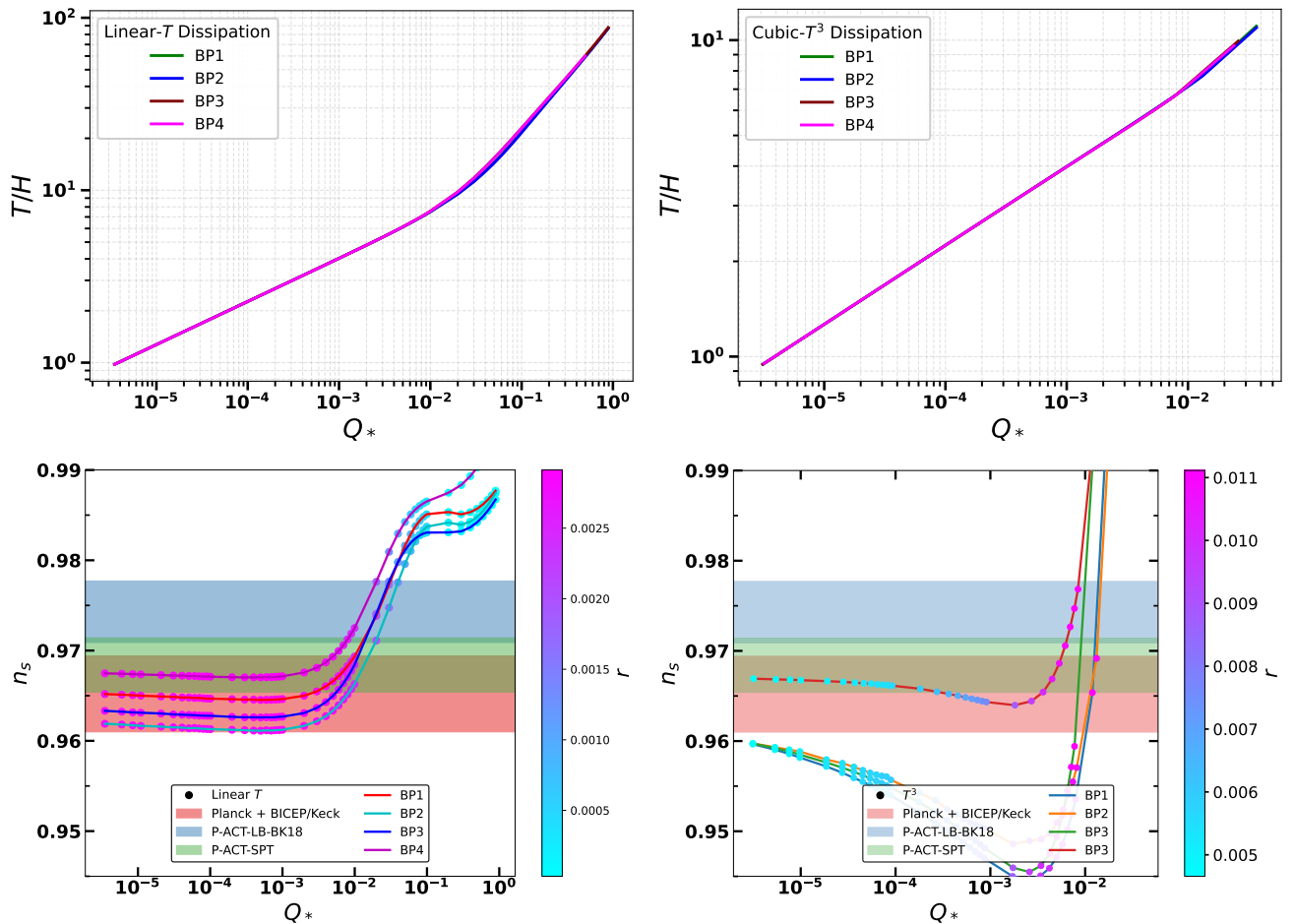


FIG. 1: The top panel shows the relationship between the dissipation ratio Q_* and the thermal ratio T_*/H_* for both linear ($\Upsilon \propto T$) and cubic ($\Upsilon \propto T^3$) dissipation regimes, whereas the bottom panel shows the scalar spectral index n_s as a function of Q_* for linear dissipation (left) and cubic dissipation (right). The color bands represent the observational constraints from *Planck+BICEP/Keck*, P-ACT-LB-BK18, and SPT datas. The four benchmark points (BP1–BP4) are indicated as colored trajectories.

As Q_* increases, dissipation becomes dynamically important. Both dissipation prescriptions exhibit a monotonic decrease in n_s with Q_* , but the rate of decrease is steeper for the cubic case due to the stronger temperature dependence. For linear dissipation, n_s enters the 95% CL region around $Q_* \sim 10^{-2}$, similarly for cubic dissipation this occurs already at $Q_* \sim 10^{-2}$. For $Q_* \gg 0.01$, both cases yield $n_s \approx 0.97$ –0.985, which is in excellent agreement with the observations of P-ACT-LB-BK18 and SPT.

The tensor-to-scalar ratio r is strongly suppressed in the warm regime; we find $r \sim 10^{-3}$ – 10^{-2} , which lies below the sensitivity thresholds of upcoming CMB experiments such as LiteBIRD and CMB-S4.

All four benchmark points produce trajectories in the n_s – Q_* plane that pass through the observationally allowed regions. This demonstrates the robustness of warm hybrid axion inflation: a wide range of dissipation strengths can yield predictions consistent with current CMB data. Notably, the cubic dissipation case allows for consistency at smaller Q_* , reducing the required dissipation strength for agreement with Planck.

Similarly in Fig. 2, we present the predictions for n_s as a function of α_s for the same four benchmark points (BP1–BP4), with observational constraints overlaid from combined datasets (P-ACT-LB-BK18).

All benchmark points yield predictions within or near the 95% confidence regions of current CMB data, which constrain $\alpha_s = -0.0041 \pm 0.0067$ [14]. The mild negative running predicted in the warm regime may be probed with future high-precision CMB and large-scale structure surveys offering a potential discriminant between cold and warm inflation scenarios.

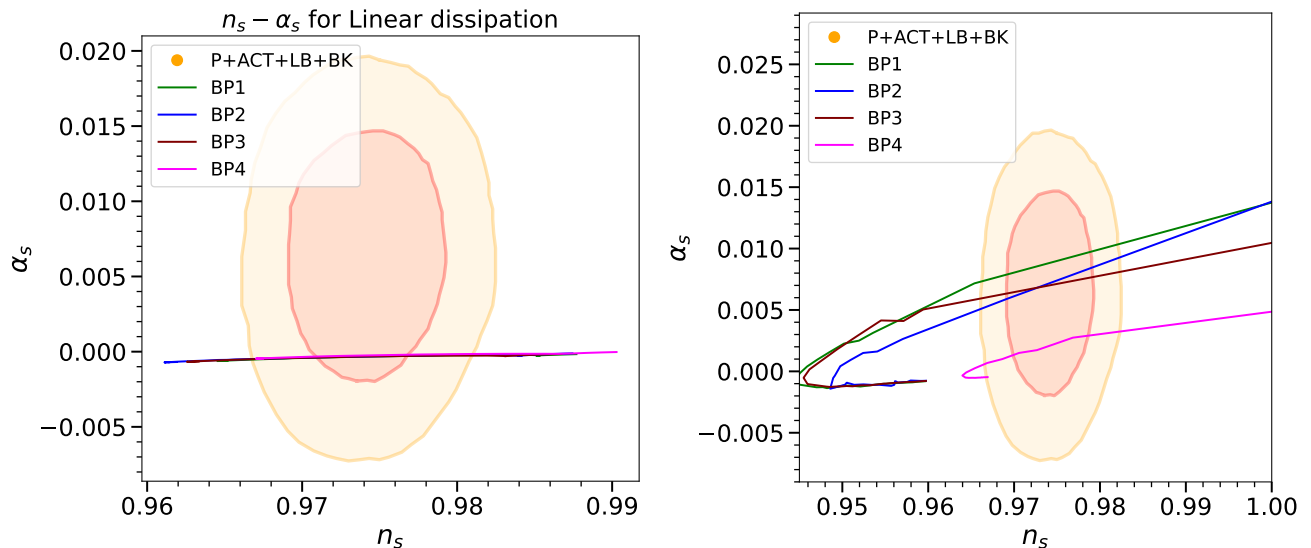


FIG. 2: Predictions for the n_s versus running of the scalar spectral index α_s for the four benchmark points (BP1–BP4) in linear dissipation (left) and cubic dissipation (right). The shaded regions correspond to the 68% and 95% confidence levels from combined CMB datasets: P-ACT-LB-BK18 .

V. CONCLUSION

In this work, we have investigated warm hybrid axion inflation within the framework of α -attractor models. We considered a two-field scenario where the inflaton is an axion-like particle with a non-canonical kinetic term, and the waterfall field is responsible for ending inflation. The warm inflation dynamics are driven by dissipative effects, characterized by a dissipation coefficient Υ , which couples the inflaton to a thermal bath. We considered two forms of the dissipation coefficient: linear ($\Upsilon \propto T$) and cubic ($\Upsilon \propto T^3$) in temperature.

Our numerical analysis, performed using the `W2easy` code, revealed that the model transitions from a cold inflation regime (disfavored by current data) to a warm inflation regime that is consistent with the latest CMB observations from Planck+BICEP/Keck, P-ACT-LB-BK18, and SPT. In particular, we found that for dissipative ratios $Q_* \gtrsim 0.01$, the scalar spectral index n_s falls within the 95% confidence region of the combined P-ACT-LB-BK18 data. The tensor-to-scalar ratio r is strongly in the warm regime, typically below $10^{-2} - 10^{-3}$, which is within the sensitivity of upcoming CMB experiments. Furthermore, the running of the scalar spectral index α_s in the strong dissipative regime is also consistent with P-ACT-LB-BK18, which may be probed by future observations.

Acknowledgment

The authors would like to thank Rudnei O. Ramos and Anish Ghoshal for their valuable discussions and constructive insights that contributed to this work. Special appreciation is extended to Rudnei O. Ramos for his assistance in clarifying the `WI2easy` framework and for his guidance on the implementation of the proposed model.

[1] Alan H. Guth. The Inflationary Universe: A Possible Solution to the Horizon and Flatness Problems. *Phys. Rev. D*, 23:347–356, 1981.

[2] Andrei D. Linde. A New Inflationary Universe Scenario: A Possible Solution of the Horizon, Flatness, Homogeneity, Isotropy and Primordial Monopole Problems. *Phys. Lett. B*, 108:389–393, 1982.

[3] Viatcheslav F. Mukhanov and G. V. Chibisov. Quantum Fluctuations and a Nonsingular Universe. *JETP Lett.*, 33:532–535, 1981.

[4] Damien A. Easson and Ruth Gregory. Circumventing the eta problem. *Phys. Rev. D*, 80:083518, 2009.

[5] Liam McAllister and Eva Silverstein. String Cosmology: A Review. *Gen. Rel. Grav.*, 40:565–605, 2008.

[6] Georges Obied, Hirosi Ooguri, Lev Spodyneiko, and Cumrun Vafa. De Sitter Space and the Swampland. 6 2018.

- [7] Prateek Agrawal, Georges Obied, Paul J. Steinhardt, and Cumrun Vafa. On the Cosmological Implications of the String Swampland. *Phys. Lett. B*, 784:271–276, 2018.
- [8] Katherine Freese, Joshua A. Frieman, and Angela V. Olinto. Natural inflation with pseudo - Nambu-Goldstone bosons. *Phys. Rev. Lett.*, 65:3233–3236, 1990.
- [9] Eva Silverstein and Alexander Westphal. Monodromy in the CMB: Gravity Waves and String Inflation. *Phys. Rev. D*, 78:106003, 2008.
- [10] Tom Rudelius. Constraints on Axion Inflation from the Weak Gravity Conjecture. *JCAP*, 09:020, 2015.
- [11] Nina K. Stein and William H. Kinney. Natural inflation after Planck 2018. *JCAP*, 01(01):022, 2022.
- [12] Renata Kallosh, Andrei Linde, and Diederik Roest. Atacama Cosmology Telescope, South Pole Telescope, and Chaotic Inflation. *Phys. Rev. Lett.*, 135(16):161001, 2025.
- [13] Ermilia Calabrese et al. The Atacama Cosmology Telescope: DR6 constraints on extended cosmological models. *JCAP*, 11:063, 2025.
- [14] Y. Akrami et al. Planck 2018 results. X. Constraints on inflation. *Astron. Astrophys.*, 641:A10, 2020.
- [15] P. A. R. Ade et al. Improved Constraints on Primordial Gravitational Waves using Planck, WMAP, and BICEP/Keck Observations through the 2018 Observing Season. *Phys. Rev. Lett.*, 127(15):151301, 2021.
- [16] Thibaut Louis et al. The Atacama Cosmology Telescope: DR6 power spectra, likelihoods and Λ CDM parameters. *JCAP*, 11:062, 2025.
- [17] A. G. Adame et al. DESI 2024 VI: cosmological constraints from the measurements of baryon acoustic oscillations. *JCAP*, 02:021, 2025.
- [18] J. A. Zebrowski et al. SPT-3G D1: Constraints on inflationary gravitational waves with two years of SPT-3G data. *Phys. Rev. D*, 112(12):123520, 2025.
- [19] D. S. Zharov, O. O. Sobol, and S. I. Vilchinskii. ACT observations, reheating, and Starobinsky and Higgs inflation. *Phys. Rev. D*, 112(2):023544, 2025.
- [20] Sergei V. Ketov, Ekaterina O. Pozdeeva, and Sergey Yu. Vernov. Inflation in $F(R)$ gravity models revisited after ACT. *JCAP*, 12:040, 2025.
- [21] Constantinos Pallis. F-Term Hybrid Inflation, Metastable Cosmic Strings and Low Reheating in View of ACT. *PoS*, CORFU2024:206, 2025.
- [22] Nobuchika Okada and Qaisar Shafi. Split supersymmetry and hybrid inflation in light of Atacama Cosmology Telescope DR6 data. 7 2025.
- [23] Constantinos Pallis. Kinetically modified Palatini inflation meets ACT data. *Phys. Lett. B*, 868:139739, 2025.
- [24] C. Pallis. ACT-inspired Kähler-based inflationary attractors. *JCAP*, 09:061, 2025.
- [25] C. Pallis. Updating GUT-Scale Pole Higgs Inflation After ACT. 10 2025.
- [26] John Ellis, Marcos A. G. Garcia, Keith A. Olive, and Sarunas Verner. Constraints on Attractor Models of Inflation and Reheating from Planck, BICEP/Keck, ACT DR6, and SPT-3G Data. 10 2025.
- [27] Qing Gao, Yungui Gong, Zhu Yi, and Fengge Zhang. Nonminimal coupling in light of ACT data. *Phys. Dark Univ.*, 50:102106, 2025.
- [28] Lang Liu, Zhu Yi, and Yungui Gong. Reconciling Higgs Inflation with ACT Observations through Reheating. 5 2025.
- [29] S. D. Odintsov and V. K. Oikonomou. Power-law $F(R)$ gravity as deformations to Starobinsky inflation in view of ACT. *Phys. Lett. B*, 870:139907, 2025.
- [30] Ioannis D. Gialamas, Alexandros Karam, Antonio Racioppi, and Martti Raidal. Has ACT measured radiative corrections to the tree-level Higgs-like inflation? *Phys. Rev. D*, 112(10):103544, 2025.
- [31] John McDonald. Unitarity-conserving nonminimally coupled inflation and the ACT spectral index. *Phys. Rev. D*, 112(12):123525, 2025.
- [32] Tanmoy Modak. R2-Higgs inflation: R3 contribution and preheating after ACT and SPT data. *Phys. Rev. D*, 112(11):115006, 2025.
- [33] Waqas Ahmed, Constantinos Pallis, and Mansoor Ur Rehman. GUT-Scale Smooth Hybrid Inflation with a Stabilized Modulus in Light of ACT and SPT Data. 10 2025.
- [34] Arjun Berera, Sudhansu Brahma, Zizang Qiu, Rudnei O. Ramos, and Gabriel S. Rodrigues. The early universe is ACT-ing warm. *JCAP*, 11:059, 2025.
- [35] Arjun Berera. The Warm Inflation Story. *Universe*, 9(6):272, 2023.
- [36] Arjun Berera. Warm inflation. *Phys. Rev. Lett.*, 75:3218–3221, 1995.
- [37] Arjun Berera. Warm inflation at arbitrary adiabaticity: A Model, an existence proof for inflationary dynamics in quantum field theory. *Nucl. Phys. B*, 585:666–714, 2000.
- [38] Arjun Berera. Warm inflation solution to the eta problem. *PoS*, AHEP2003:069, 2003.
- [39] Arjun Berera. Interpolating the stage of exponential expansion in the early universe: A Possible alternative with no reheating. *Phys. Rev. D*, 55:3346–3357, 1997.
- [40] Rudnei O. Ramos and L. A. da Silva. Power spectrum for inflation models with quantum and thermal noises. *JCAP*, 03:032, 2013.
- [41] Gabriel S. Rodrigues and Rudnei O. Ramos. WI2easy: warm inflation dynamics made easy. *JCAP*, 09:014, 2025.
- [42] Meysam Motaaharfar, Vahid Kamali, and Rudnei O. Ramos. Warm inflation as a way out of the swampland. *Phys. Rev. D*, 99(6):063513, 2019.
- [43] Arjun Berera and Jaime R. Calderón. Trans-Planckian censorship and other swampland bothers addressed in warm inflation. *Phys. Rev. D*, 100(12):123530, 2019.
- [44] Andrei D. Linde. Hybrid inflation. *Phys. Rev. D*, 49:748–754, 1994.

- [45] Waqas Ahmed, Anish Ghoshal, and Umer Zubair. Primordial black holes and second-order gravitational waves in axionlike hybrid inflation. *Phys. Rev. D*, 112(6):063512, 2025.
- [46] Matteo Braglia, Andrei Linde, Renata Kallosh, and Fabio Finelli. Hybrid α -attractors, primordial black holes and gravitational wave backgrounds. *JCAP*, 04:033, 2023.
- [47] Renata Kallosh and Andrei Linde. On the present status of inflationary cosmology. *Gen. Rel. Grav.*, 57(10):135, 2025.
- [48] Mario Galante, Renata Kallosh, Andrei Linde, and Diederik Roest. Unity of Cosmological Inflation Attractors. *Phys. Rev. Lett.*, 114(14):141302, 2015.
- [49] Anish Ghoshal and Alessandro Strumia. Traversing a kinetic pole during inflation: primordial black holes and gravitational waves. *JCAP*, 07:011, 2024.
- [50] Micol Benetti and Rudnei O. Ramos. Warm inflation dissipative effects: predictions and constraints from the Planck data. *Phys. Rev. D*, 95(2):023517, 2017.
- [51] Vahid Kamali, Meysam Motaharfar, and Rudnei O. Ramos. Recent developments in warm inflation. *Universe*, 9(3), 2023.
- [52] Kim V. Berghaus, Peter W. Graham, David E. Kaplan, Guy D. Moore, and Surjeet Rajendran. Dark energy radiation. *Phys. Rev. D*, 104(8):083520, 2021.
- [53] Mar Bastero-Gil, Arjun Berera, Rudnei O. Ramos, and Joao G. Rosa. Warm Little Inflaton. *Phys. Rev. Lett.*, 117(15):151301, 2016.
- [54] Ian G. Moss and Chun Xiong. On the consistency of warm inflation. *JCAP*, 11:023, 2008.